IEEE Access
Multidisciplinary | Rapid Review | Open Access Journal

Received September 30, 2019, accepted October 11, 2019, date of publication October 14, 2019, date of current version October 25, 2019.

Digital Object Identifier 10.1109/ACCESS.2019.2947303

All-Optical Multilevel Amplitude Regeneration Based on Polarization-Orthogonal Continuous-Wave-Light-Assisted Nonlinear-Optical Loop Mirror (PC-NOLM) Subsystem

BIAO GUO, FENG WEN, BAOJIAN WU, FAN SUN, AND KUN QIU

Key Laboratory of Optical Fiber Sensing and Communications, Ministry of Education, University of Electronic Science and Technology of China, Chengdu 611731, China

Corresponding author: Baojian Wu (bjwu@uestc.edu.cn)

This work was supported in part by the National Natural Science Foundation of China under Grant 61671108 and Grant 61975027, in part by the General Project of Sichuan Provincial Education Department under Grant 18ZB0235, in part by the Marie Skłodowska-Curie Actions under Grant 701770-INNOVATION, and in part by the 111 Project under Grant B14039.

ABSTRACT We demonstrate a multilevel amplitude regeneration experiment for non-return-to-zero 4-level pulse amplitude modulated (NRZ-PAM4) signals in the proposed polarization-orthogonal continuous-wave-light-assisted nonlinear-optical loop mirror (PC-NOLM) subsystem. A uniform regenerative behavior including the same noise-suppression efficiency and the noise-handling capability is observed across multiple amplitude levels. The pre-phase modulation is carried out for the input signal enabling the multilevel amplitude regeneration directly on highly-spectral-efficient modulated formats. An overall improvement of 2.33 dB is achieved by optimizing the launched optical power and the distortion strength in the all-optical NRZ-PAM4 regeneration experiment. The uniform regenerative performance for the proposed PC-NOLM regenerator is also analyzed numerically to reveal the regenerative mechanism and the influence from the operational parameters.

INDEX TERMS All-optical signal regeneration, optical fiber communication, optical signal processing, fiber nonlinear optics, nonlinear optical devices.

I. INTRODUCTION

All-optical signal regeneration is the key technology to improve the system capacity and transparent reach for the long-haul fiber communication networks [1], [2]. To meet the regenerative requirement of advanced modulation formats, all-optical regeneration technology should support multilevel phase and amplitude operations. Employing a phase sensitive amplifier (PSA), a 6-order phase quantization has been implemented in a coherent parametric mixer [3]. Furthermore, the multi-channel operation has also been demonstrated using pump-wavelength optimization [4], polarization-orthogonal pump [5], or optical time lens schemes [6]. Additionally, the pump power that was required in the multilevel phase regeneration could been reduced in a vector PSA process [7]. On the other hand, the nonlinear-optical loop mirror (NOLM) is a promising technology to perform all-optical amplitude regeneration through its well-known power oscillatory behavior [8]. By cascading three-stage NOLMs a high bit rate-160Gb/s all-optical regeneration and de-multiplexing have been experimentally demonstrated, but only working on the simple data format [9]. For those advanced modulated formats, a single NOLM for the 4-level pulse amplitude modulated signal (PAM4) in our previous work [10] and a modified NOLM for the star 8-level quadrature amplitude modulated signal (star-8QAM) [11] have been experimentally achieved. Even for higher constellation orders, i.e. QAM256 signals the NOLM-based regenerative Fourier transformation scheme was theoretically proposed to perform the dual-quadrature operation [12]. However, these

The associate editor coordinating the review of this manuscript and approving it for publication was Chao Zuo.

conventional NOLM regenerators are based on the self-phase modulation (SPM) effect, and consequently leading to a strong oscillatory strength on high launched powers [9], [13], which gives a severe degradation on the regeneration performance of high-order amplitude levels. To address this issue, we demonstrate a polarization-orthogonal continuous-wave-light-assisted NOLM (PC-NOLM) regenerator to achieve the uniform amplitude-noise suppression on each level. Compared to the conventional NOLM regenerator [11], [21], we only add a CW source as an assisted light in the proposed unit and significantly improve the regenerative range especially on high amplitude levels. Therefore, more quality improvement of 2.33dB is achieved by the proposed PC-NOLM compared to only 0.92dB in the conventional unit [10].

In this paper, the proposed multilevel amplitude regenerator is still based on a single NOLM unit, but with two orthogonally-polarized-wave inputs: a CW-assisted light and a signal as pump. The CW-assisted light is launched into the input port of the NOLM unit. But on the other hand, the signal pump is only injected into the clockwise-propagating arm to introduce an additional cross-phase modulation (XPM)-induced nonlinear phase shift (NPS) to the CW-assisted light. This operation gives a uniform regenerative behavior on multiple levels. Moreover, the regenerator working as an in-line element can significantly improve the system's transmission reach [14]. Our proposed PC-NOLM regenerator is also designed for this purpose. A 1.3dB SNR improvement has been obtained through our simulation suggesting a reach extension by the regenerator. In the experiment, we carried out a pre-phase modulation for the input signal significantly increasing the SBS threshold of highly nonlinear fiber (HNLF) used in the PC-NOLM regenerator. Therefore, we could achieve the multilevel amplitude regeneration directly on the highly-spectral-efficient modulated signals, which was non-return-to-zero (NRZ)-PAM4 in the experiment. The rest of the paper is organized as follows: Section II introduces the theoretical model of the proposed regenerator, and analyzes the characteristics of the power transfer function (PTF); Section III carries out the experimental investigations on the PTF measurement, the uniform regenerative performance on each level and the multilevel amplitude regeneration of NRZ-PAM4 signals; finally, in section IV, we draw the conclusions of the paper.

II. THEORETICAL MODEL

The proposed PC-NOLM regenerator including two optical couplers (OC1 and OC2) and a HNLF is depicted in Fig. 1. The CW-assisted light was input into the NOLM structure through OC1, and then split into two counter-propagating waves acquiring a nonlinear phase difference from the SPM and XPM effects in HNLF. A signal pump was injected into the clockwise-propagating arm of the NOLM structure through OC2, which introduced not only the SPM-induced NPS to itself, but also the XPM-induced NPS to the CW-assisted light. To achieve the uniform regenerative operation,

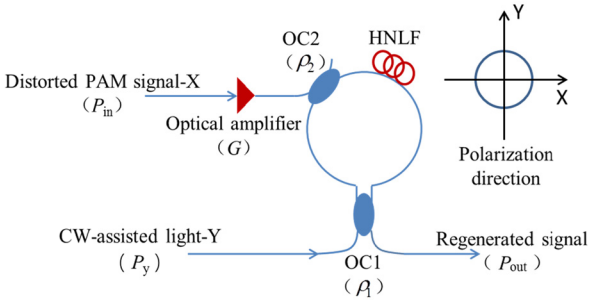

FIGURE 1. The structure of the PC-NOLM regenerator.

the signal pump and the CW-assisted light have the same wavelength, but the orthogonal states of polarization (SOP). In the paper, we assumed an X-linearly-polarized signal and a Y-linearly-polarized CW light. The regenerated signal containing the interfering light between two counter-propagating CW-assisted waves as well as the signal pump, was collected at the transmission port of the NOLM unit. Following the methodology of [15]–[17], we derived the output powers of the signal P^x_{out} and the assisted light P^y_{out}:

$$P^x_{\text{out}} = 10^{-\alpha_{\text{dB}}L/10}\rho_2(1-\rho_1)GP_{\text{in}} \tag{1.1}$$

$$P^y_{\text{out}} = 10^{-\alpha_{\text{dB}}L/10}\rho_2 P_y[\rho_1^2 + (1-\rho_1)^2 - 2\rho_1(1-\rho_1)\cos(\Delta\phi)] \tag{1.2}$$

where α_{dB}, γ, and L are the loss coefficient, nonlinear coefficient and length of the HNLF, respectively; $L_{\text{eff}} = (1-e^{-\alpha L})/\alpha$ is the effective length; ρ_1 and ρ_2 are the coupling ratios of OC1 and OC2; G is the gain coefficient of the optical amplifier that boosts the input signal; P_{in} and P_y are the input powers of the signal and the CW-assisted light; $\Delta\phi = 2\gamma P_{\text{in}}L_{\text{eff}}G(1-\rho_2)/3$ represents the nonlinear phase difference, and the coefficient 2/3 comes from the nonlinear effect between two orthogonally-polarized waves [18]. A cosine- function power oscillatory behavior as shown in Eq. (1.2) was expected from the output CW-assisted light, due to the nonlinear phase difference between the two counter-propagating CW waves. Then we obtained the total output power of the proposed PC-NOLM regenerator as follows:

$$P_{\text{out}} = 10^{-\alpha_{\text{dB}}L/10}[\rho_1^2\rho_2 P_y + (1-\rho_1)^2\rho_2 P_y + \rho_2(1-\rho_1)GP_{\text{in}} - 2\rho_1(1-\rho_1)\rho_2 P_y\cos(\Delta\phi)] \tag{2}$$

Equation (2) reveals the nonlinear behavior achieved in the proposed single NOLM unit. The new structure leads to a change on the NOLM's transmission response corresponding to the fourth term $\sim P_y cos\,(c \cdot P_{in})$, different from the conventional NOLM regenerator with the response of $\sim P_{in} cos\left(c' \cdot P_{in}\right)$ [10], [11], where the constant c and c' are related to the structure parameters. This change gives an equal power-spacing between two adjacent working points (WPs) and also the same oscillatory strength in each period, enabling the uniform regeneration on multiple levels. The typical PTF curve (red line) and its slope (green line) are depicted in Fig. 2.

To identify the WP and the regenerative region (RR) corresponding to each level, we respectively calculated the slopes

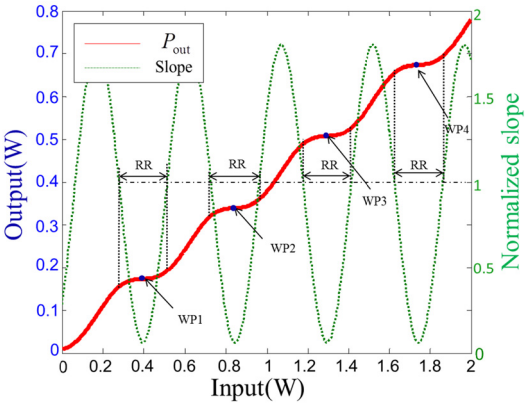

FIGURE 2. PTF result and its slope achieved by the PC-NOLM regenerator.

d_x and d_y for the output signal and the output CW-assisted light. Therefore the total slope d of the PC-NOLM regenerator was given as:

$$\begin{aligned} d &= d_x + d_y \\ &= 10^{-\alpha_{\mathrm{dB}}L/10}(1-\rho_1)\rho_2 G[1+\frac{4}{3}(1-\rho_2)\rho_1\gamma \\ &\quad \times P_y L_{eff}\sin(-\Delta\varphi_y)] \end{aligned} \tag{3}$$

We define the best noise-suppression point as the WP in each period, i.e. the total slope of output power $d = 0$, which gives to the WP for m-th level:

$$P_{in} = \frac{3m\pi}{\gamma LG(1-\rho_2)} \tag{4}$$

A constant oscillation period of $T = 3\pi/\gamma LG(1-\rho_2)$ was achieved as we predicted from Eq. (2). The RR of each level was also determined through $|d| < 1$ where the noise suppression happens:

$$P_{in} \in \left[\frac{3(4m-1)\pi}{4\gamma LG(1-\rho_2)}, \frac{3(4m+1)\pi}{4\gamma LG(1-\rho_2)}\right] \tag{5}$$

Obviously, the width of the RRs, i.e. the noise-handling capability for all levels is equal, further confirming the uniform regenerative concept of the PC-NOLM subsystem.

III. EXPERIMENTAL SETUP AND RESULTS

The uniform multilevel amplitude regeneration experiment was carried out in the proposed PC-NOLM subsystem, as depicted in Fig. 3. At the transmitter we generated the NRZ-PAM4 signal and the CW-assisted light as follows: A CW light with the wavelength of 1550nm was firstly launched into a phase-modulator (PM) which was driven by a 12.5Gb/s pseudo random binary sequence (PRBS) NRZ signal, and then split into two orthogonally-polarized waves by a polarization beam splitter (PBS). One part of the waves as a CW-assisted light was input into the NOLM unit through OC1, which power was amplified to 0.2W by an Erbium-doped fiber amplifier (EDFA2). The other part was injected into an intensity modulator (IM) for the optical PAM4 generation. The intensity modulator is a ''modulator box'' which includes a RF amplifier to control the strength of the input electrical signal and consequently effecting the modulation depth of the optical modulator. The modulator IM1 was driven by an NRZ-PAM4 electrical signal generated by a NRZ-to-PAM4 convertor [19]. Therefore a clean NRZ-PAM4 signal was obtained for the multilevel amplitude operation of the PC-NOLM regenerator. To evaluate the regenerative behavior, the NRZ-PAM4 signal was then degraded through a distortion loading unit, which included an optical modulator (IM2) and a pulse pattern generator (PPG2). A 9.8Gb/s PRBS-NRZ signal generated by PPG2 introduced an amplitude distortion into the clean signal, which strength was controlled by tuning the RF gain in IM2. After the power amplification in EDFA1 the NRZ-PAM4 signal as the pump was launched into the NOLM unit through OC2. The optical isolator (ISO) was used to prevent any unwanted feedback-light into the transmitter. To maintain the orthogonally polarized relationship between the input signal and the CW-assisted light, two polarization controllers (PC2 and PC3) were placed at the input ports of the couplers. The NOLM unit was comprised of a 50:50 OC1, a PC4, a 2.9km-length HNLF and a 75:25 OC2. The nonlinear coefficient of the HNLF was 10.8 W^{-1}/km and the loss factor was 0.7 dB/km. The total loss of other parts (including the power splitting from OCs) was 8dB. The PC used in the NOLM unit was to optimize the initial state of the interferometer. At the transmission port, the regenerated signal was collected by a 50G optical photodiode (PD). The received electrical signal was sampled by a sampling oscilloscope (Tektronix, DSA8300). We recorded the data at the widest eye-opening and reconstructed the results by using the Matlab function ''eyesight (P_{out}, 2)'', where ''2'' in the function represents the figure containing two eyes.

We firstly measured the PTF curve of the proposed PC-NOLM regenerator to locate the WPs of all levels. To this end, a CW pump as the signal was directly input to the NOLM without any intensity modulation, i.e. bypassing the modulators IM1 and IM2 in Fig. 3. We used a long-HNLF to significantly reduce the optical powers of the WPs. Meanwhile we carried out the pre-phase modulation to the input signal for increasing the SBS threshold of HNLF, enabling a highly effective launched-power. In the experiment, we changed the signal power from 0.1W to 2W and kept a constant CW-assisted light of 0.2W. To improve the reliability of experimental data, we recorded 50 samples within 10s for each point. Figure 4 depicts the measured PTF curve with the error bar for the PC-NOLM regenerator. A staircase-like PTF with four power-plateau regions was obtained in the optimized NOLM unit. Four WP points were respectively at 0.46W, 0.92W, 1.38W and 1.84W, corresponding to the definition of the total slope $d = 0$, as given by Eq. (4). An equal power-spacing of 0.46W was achieved confirming the uniform regenerative concept of the proposed regenerator. According to the definition of RR in Eq. (5), we measured the RR corresponding to each WP, i.e. around 0.23W in our case. Within this RR the regeneration gain was achieved. We noticed that the RR has covered 50% of

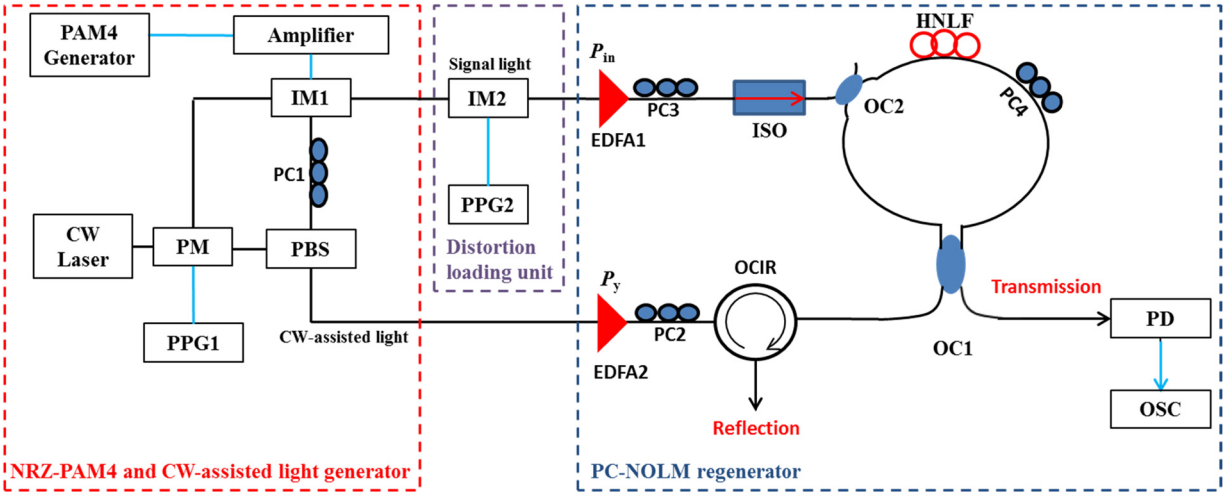

FIGURE 3. Experimental setup of the all-optical NRZ-PAM4 regeneration in the PC-NOLM subsystem.

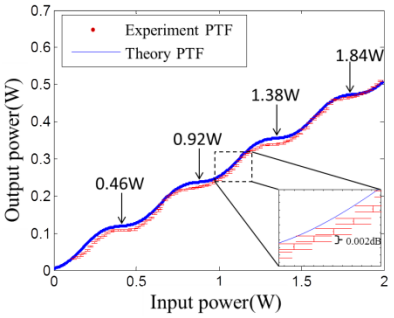

FIGURE 4. PTF results for the PC-NOLM regenerator.

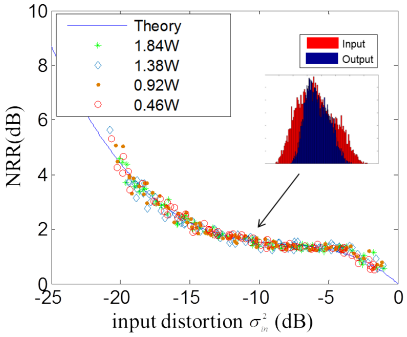

FIGURE 5. NRR results for each WP and distribution diagram obtained at the input distortion of −10dB.

the power spacing demonstrating the large noise handling capability and the high toleration of power level shifting. Moreover, the small error bar, i.e. around 0.002dB depicted in the inset of Fig. 4 proves the stability of the output power from the PC-NOLM subsystem. We also calculated the theoretical results using Eq. (2), referring to the blue line in Fig. 4. A good agreement between theory and experiment was observed for the whole curve. The results also show that a high optical power launched into the HNLF, which proves the pre-phase modulation operation works in the proposed structure.

Subsequently, we investigated the noise suppression performance on each WP. Specifically, we input a 10Gb/s PRBS-NRZ signal as the pump, which was distorted by an electrical 9.8Gb/s PRBS-NRZ signal through IM2. The strength was controlled by tuning the RF gain of the electrical signal from 0 to 25dB. In the experiment we respectively kept the input average optical power at 0.23W, 0.46W, 0.69W and 0.92W in order to let the "1" level of the input NRZ signals fall on every WP point. Then we measured the amplitude noise of the output signals as a function of the distortion strength. The amplitude regeneration performance was quantified by the normalized noise reduction ratio (NRR) [20]:

$$NRR_l = \sigma_{\text{in},l}^2 \Big/ \sigma_{\text{out},l}^2 \tag{6}$$

where $\sigma_{\text{in},l}^2 = E\left[(x - x_l)^2\right]/\Delta x^2$ represents the input noise of the l-th level normalized to the amplitude spacing $x = x_l - x_{l-1}$, and x_l is the amplitude of the l-th WP; $\sigma_{\text{out},l}^2 = E\left[(y - y_l)^2\right]/\Delta y^2$ is the output noise of each level normalized to the output spacing $y = y_l - y_{l-1}$, and y_l is the corresponding output obtained at x_l; x and y are the measured input and output amplitude, respectively. Figure 5 depicts the NRR results versus input noise at four WPs. Here we only considered the amplitude distortion on the "1" level of NRZ signals which performed the noise suppression in power-plateau regions. It can be observed that the noise suppression performance including the handling capability of input noise and the noise-suppression efficiency are identical for all WPs, which means the uniform regenerative behavior can be achieved on multiple levels in the proposed PC-NOLM regenerator. From Fig. 5, the NRR drops down with the increase of the input distortion strength, which defines the noise-handling capability, i.e. RR of the regenerator. A better noise-suppression efficiency can be obtained at the lower launched distortion due to the small slope value obtained around WPs, see the green line in Fig. 2. In Fig. 5, the theoretical curve (blue line) calculated from Eq. (6) was plotted as well, and the agreement between the theoretical and experimental results is illustrated. The noise suppression function

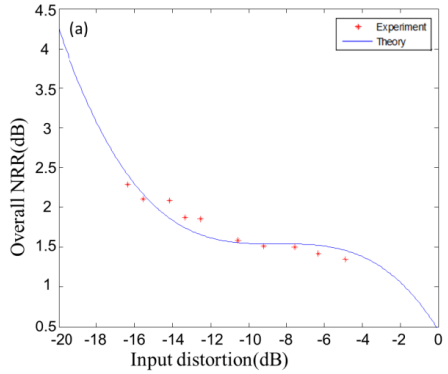

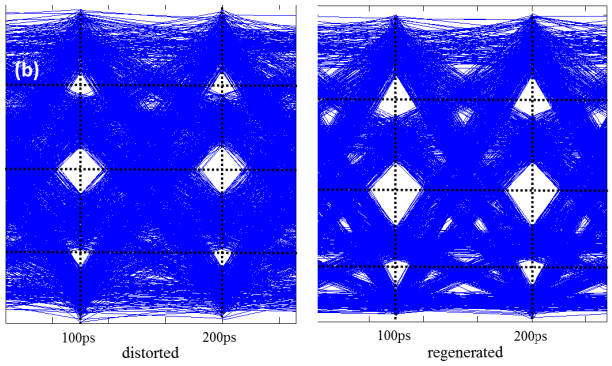

FIGURE 6. (a) Overall NRR improvement achieved by the NRZ-PAM4 signal regeneration and (b) distorted and regenerated eye diagrams at the NRRoverall = 1.67.

for the PC-NOLM subsystem can also be seen from the power histogram inserted in Fig. 5, corresponding to the case with the input distortion of −10dB at the WP of 0.46W.

Finally, we carried out the multilevel amplitude regeneration of NRZ-PAM4 signals in the PC-NOLM subsystem. As the same as our previous test, a degraded optical NRZ-PAM4 signal with the average optical power of about 29.7dBm was launched into the NOLM, and all of the input levels located at the corresponding power-plateau regions. We used the overall NRR to evaluate the regeneration performance by the following definition:

$$\frac{1}{NRR_{overall}} = \frac{1}{M}\sum_{l}^{M}\frac{1}{NRR_l} \tag{7}$$

where NRR_l represents the NRR at level l, and M is the level number. The measured overall NRR results are shown in Fig. 6(a), along with the theoretical curve similar to that of Fig. 5, which can be explained from the uniform regenerative behavior on each level. In our experiment, a maximal $NRR_{overall}$ improvement of 2.33dB was achieved at the input distortion of −17.1dB. We also compared the eye diagrams of the distorted and regenerated signals when $NRR_{overall}$ = 1.67dB, as shown in Fig. 6(b). These two eyes were reconstructed through the received data sampled by the sampling

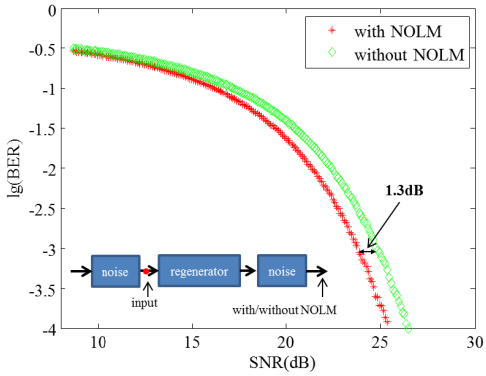

FIGURE 7. The BER results in the PC-NOLM transmission link.

oscilloscope, only for a visual demonstration of signals before and after the regenerator. The regenerated NRZ-PAM4 signal has a larger eye opening confirming a four-level amplitude regeneration happened in the proposed PC-NOLM subsystem. In principle, the amplitude regeneration of a higher-order PAM signal may be expected by using a longer HNLF or increasing the launched optical power.

To further investigate the regenerative effect on the long-haul transmission link, we carried out the Monte Carlo simulation to evaluate the regenerative performance through direct error counting. In the numerical calculations, the experimentally verified transfer function of the regenerator was used. We inserted the regenerator into the middle of the transmission link, working as an in-line element [14]. For this case a 1.3dB SNR improvement was obtained by using the PC-NOLM regenerator compared to the un-regenerative case, suggesting a reach extension in the PC-NOLM-based transmission link. This PAM4 operation has demonstrated the multilevel amplitude regeneration capability. In the future investigation, we will use the proposed PC-NOLM regenerator to deal with high-order QAM signals for the long-haul transmission. In that case, the all-optical regeneration technology has more advantages on bandwidth, cost and power consumption compared to the current DSP-based signal processing unit.

IV. CONCLUSION

We have proposed a novel PC-NOLM subsystem and demonstrated, to the best of our knowledge, the first regenerative experiment on the NRZ-PAM4 signal. The new structure performed the uniform regenerative behavior on multiple levels, achieving the same noise-suppression efficiency and noise-handling capability to every WP. The use of the pre-phase modulation significantly increased the effectively launched optical power, enabling all-optical signal regeneration on NRZ-based highly-spectral-efficient modulated formats. The maximum NRR improvement of 2.33 dB was achieved in the experiment by simultaneously suppressing the amplitude distortion on four levels. Through the numerical simulations, a 1.3dB SNR improvement was achieved

compared to the un-regenerative case suggesting a reach extension in the PC-NOLM-based transmission link.

REFERENCES

[1] M. A. Sorokina and S. K. Turitsyn, "Regeneration limit of classical Shannon capacity," *Nature Commun.*, vol. 5, p. 3861, May 2014.
[2] A. E. Willner, S. Khaleghi, M. R. Chitgarha, and O. F. Yilmaz, "All-optical signal processing," *J. Lightw. Technol.*, vol. 32, no. 4, pp. 660–680, Feb. 15, 2014.
[3] R. Slavík, F. Parmigiani, J. Kakande, C. Lundström, M. Sjödin, P. A. Andrekson, R. Weerasuriya, S. Sygletos, A. D. Ellis, L. Grüner-Nielsen, D. Jakobsen, S. Herstrøm, R. Phelan, J. O'Gorman, A. Bogris, D. Syvridis, S. Dasgupta, P. Petropoulos, and D. J. Richardson, "All-optical phase and amplitude regenerator for next-generation telecommunications systems," *Nature Photon.*, vol. 4, pp. 690–695, Sep. 2010.
[4] S. Sygletos, P. Frascella, S. K. Ibrahim, L. Grüner-Nielsen, R. Phelan, and J. O'Gorman, and A. D. Ellis, "A practical phase sensitive amplification scheme for two channel phase regeneration," *Opt. Express*, vol. 19, no. 26, pp. 938–945, 2011.
[5] F. Parmigiani, G. D. Hesketh, R. Slavik, P. Horak, P. Petropoulos, and D. J. Richardson, "Polarization-assisted phase-sensitive processor," *J. Lightw. Technol.*, vol. 33, no. 6, pp. 1166–1174, Mar. 15, 2015.
[6] P. Guan, F. D. Ros, M. Lillieholm, N.-K. Kjøller, H. Hu, K. M. Røge, M. Galili, T. Morioka, and L. K. Oxenløwe, "Scalable WDM phase regeneration in a single phase-sensitive amplifier through optical time lenses," *Nature Commun.*, vol. 9, no. 1, p. 1049, 2018.
[7] Z. Xing, H. Wang, and Y. Ji, "QPSK signal regeneration based on vector phase sensitive amplification with low pump powers," *IEEE Access*, vol. 7, pp. 63936–63943, 2019.
[8] N. J. Doran and D. Wood, "Nonlinear-optical loop mirror," *Opt. Lett.*, vol. 13, no. 1, pp. 56–58, 1988.
[9] A. Bogoni, P. Ghelfi, M. Scaffardi, and L. Poti, "All-optical regeneration and demultiplexing for 160-gb/s transmission systems using a NOLM-based three-stage scheme," *IEEE J. Sel. Topics Quantum Electron.*, vol. 10, no. 1, pp. 192–196, Jan./Feb. 2004.
[10] F. Wen, C. P. Tsekrekos, Y. Geng, X. Zhou, B. Wu, K. Qiu, S. K. Turitsyn, and S. Sygletos, "All-optical multilevel amplitude regeneration in a single nonlinear optical loop mirror," *Opt. Express*, vol. 26, no. 10, pp. 12698–12706, 2018.
[11] T. Roethlingshoefer, T. Richter, C. Schubert, G. Onishchukov, B. Schmauss, and G. Leuchs, "All-optical phase-preserving multilevel amplitude regeneration," *Opt. Express*, vol. 22, no. 22, pp. 27077–27085, 2014.
[12] M. Sorokina, S. Sygletos, A. Ellis, and S. Turitsyn, "Regenerative Fourier transformation for dual-quadrature regeneration of multilevel rectangular QAM," *Opt. Lett.*, vol. 40, no. 13, pp. 3117–3120, 2015.
[13] O. Pottiez, B. Ibarra-Escamilla, and E. A. Kuzin, "Large amplitude noise reduction in ultrashort pulse trains using a power-symmetric nonlinear optical loop mirror," *Opt. Laser Technol.*, vol. 41, no. 4, pp. 384–391, Jun. 2009.
[14] S. L. I. Olsson, H. Eliasson, E. Astra, M. Karlsson, and P. A. Andrekson, "Long-haul optical transmission link using low-noise phase-sensitive amplifiers," *Nature Commun.*, vol. 9, no. 1, p. 2513, 2018.
[15] W. Astar, C. C. Wei, Y.-J. Chen, J. Chen, and G. M. Carter, "Polarization-insensitive, 40 Gb/s wavelength and RZ-OOK-to-RZ-BPSK modulation format conversion by XPM in a highly nonlinear PCF," *Opt. Express*, vol. 16, no. 16, pp. 12039–12049, 2008.
[16] K. Croussore, C. Kim, and G. Li, "All-optical regeneration of differential phase-shift keyed signals based on phase-sensitive amplification," *Proc. SPIE*, vol. 5814, pp. 166–175, May 2005.
[17] K. Ikeda, J. M. Abdul, H. Tobioka, T. Inoue, S. Namiki, and K. Kitayama, "Design considerations of all-optical A/D conversion: Nonlinear fiber-optic Sagnac-loop interferometer-based optical quantizing and coding," *J. Lightw. Technol.*, vol. 24, no. 7, pp. 2618–2628, Jul. 2006.
[18] G. P. Agrawal, *Nonlinear Fiber Optics*. Beijing, China: Publishing House of Electronics Industry, 2010, pp. 134–165.
[19] F. Wen, S. Sygletos, C. P. Tsekrekos, X. Zhou, Y. Geng, B. Wu, K. Qiu, and S. K. Turitsyn, "Multilevel power transfer function characterization of nonlinear optical loop mirror," in *Proc. 19th Int. Conf. Transparent Opt. Netw. (ICTON)*, Jul. 2017, pp. 1–4.
[20] X. Kong, B. Wu, X. Zhou, Q. Wan, S. Jiang, F. Wen, and K. Qiu, "Design of all-optical multi-level regenerators based on Mach–Zehnder interferometer," *Optics Commun.*, vol. 380, pp. 377–381, Dec. 2016.
[21] F. Wen, B. Wu, K. Qiu, and S. Sygletos, "Conjugate nonlinear-optical loop mirror (Conj-NOLM)-based phase-preserving multilevel amplitude regenerator," *Opt. Express*, vol. 27, no. 14, pp. 19940–19949, 2019.

BIAO GUO received the B.S. degree from the University of Electronic Science and Technology of China, in 2016, where he is currently pursuing the Ph.D. degree with the Key Laboratory of Optical Fiber Sensing and Communications, Ministry of Education, School of Information and Communication Engineering. His research interests include all-optical signal processing and optical nonlinearity effect.

FENG WEN received the Ph.D. degree from the University of Electronic Science and Technology of China, in 2013, where he is currently a Lecturer. He has recently carried out research on all-optical regeneration, amplification, reserve cell computing, and silicon-based photonic functional chips based on the non-linear effect of optical fibers. He is a member of the International Institute of Electrical and Electronic Engineers and the American Optical Society. He reviews manuscripts for many academic journals and conferences, such as *Optics Communications*, *Optical Fiber Technology*, and IEEE CIC ICCC.

BAOJIAN WU received the Ph.D. degree from Shanghai Jiaotong University, in 1999. He is currently a Professor with the Key Laboratory of the Ministry of Optical Fiber Sensing and Communication Education, College of Communication and Information Engineering, University of Electronic Science and Technology of China. He mainly involved in the teaching and scientific research of optical fiber communication, intelligent optical information processing, and microwave photonics.

FAN SUN received the B.S. degree from Shangqiu University, in 2014, where she is currently pursuing the Ph.D. degree with the Key Laboratory of Optical Fiber Sensing and Communications, Ministry of Education, School of Information and Communication Engineering. Her research interests include all-optical signal processing and optical nonlinearity effect.

KUN QIU received the Ph.D. degree from Tsinghua University, in 1990. He is currently a Professor and the Team Leader of the Key Laboratory of the Ministry of Optical Fiber Sensing and Communication Education, College of Communication and Information Engineering, University of Electronic Science and Technology of China. His researches mainly include MIMO radar signal detection theory, weak target detection in complex Gauss clutter, adaptive waveform design, and other fields.